Constrained Optimum Photovoltaic Generation Dispatch for Energy Bill Minimization

Gabriel Sousa*, Jean Patric da Costa†, Emerson Giovani Carati‡,
Rafael Cardoso§ and Carlos Marcelo de Oliveira Stein¶
Programa de Pós-Graduação em Engenharia Elétrica
Universidade Tecnológica Federal do Paraná
Pato Branco, Brasil
*sousa@alunos.utfpr.edu.br, †jpcosta@utfpr.edu.br, ‡emerson@utfpr.edu.br,
§rcardoso@utfpr.edu.br, ¶cmstein@utfpr.edu.br

***Abstract*—This paper proposes a new photovoltaic generation dispatch method based on Lagrange multiplier. Initially, a microgrid model is derived from power flux equations. Then, a performance index based on Brazilian regulation is developed. Finally, a cost function design procedure that guarantees the optimum photovoltaic generation dispatch and energy bill minimization is presented in detail. It is demonstrated that a very fast convergence can be obtained with the proposed optimization algorithm, which improves the response of the grid connected PV systems. Simulation results are given to support the theoretical analysis and to illustrate the performance of PV generation dispatch with the proposed optimization algorithm.**

***Index Terms*—Microgrids, Reactive Power, Economical Dispatch, Constrained Optimization.**

I. Introduction

The increasing demand for energy, the environmental impacts and the limited amount of fossil fuels, motivate the intensive use of renewable sources, especially the photovoltaic generation for its ease of implantation in urban environments, proving a viable source of energy for the use in microgrids [1], [2], [3].

In microgrids, as shown in Fig. 1, the presence of generating elements makes it possible to partially or totally supply the loads only by renewable sources, reducing the import of energy from the utility grid, making these sources economically interesting. However, uncontrolled power supply can cause problems in power quality, especially the power factor, which can degrade when there is only active power dispatch [4], [5].

This can lead to penalties on the electric bill, which can difficult the return on investment.

This paper proposes a method for control the active and reactive power dispatch, weighting the effort between two objectives: supply the loads and avoid fines due to the low power factor.

II. The model and its restrictions

To simplify the analysis, the microgrid was modeled neglecting the losses due to transmission. All the loads and distributed generators, as shown in Fig. 1, are grouped in two elements, then the power imported from grid can be expressed as:

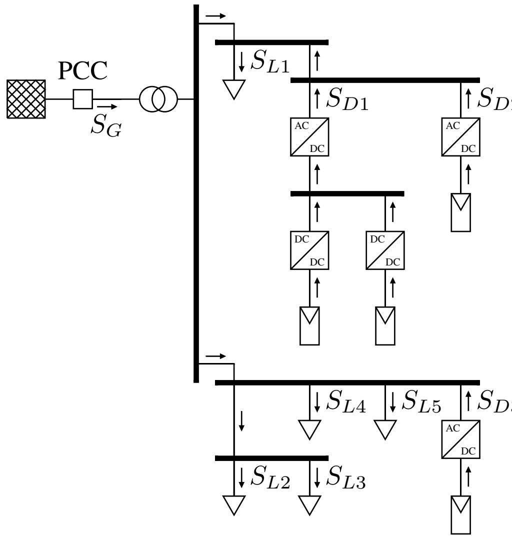

Fig. 1: Simplified block diagram microgrid with photovoltaic generation units.

$$S_G = S_L - S_d \xrightarrow{S_x = P_x + \jmath Q_x} \begin{cases} P_G = P_L - P_D \\ Q_G = Q_L - Q_D \end{cases} . \quad (1)$$

The maximum apparent power that the set of distributed generators can dispatch are limited to the region:

$$\mathcal{G} = \left\{ (P_D, Q_D) \in \mathbb{R}^2 \mid \sqrt{P_D^2 + Q_D^2} \le S_{\max} \right\}, \quad (2)$$

where P_D and Q_D are the active and reactive power injected delivered by the generation set.

Due to the nature of some renewable resources, the power available at the primary source can vary and, as a consequence, limits the capacity of active power injection by the generating unit. This constraint is defined as:

$$\mathcal{T} = \left\{ (P_D, Q_D) \in \mathbb{R}^2 \mid 0 \le P_D \le P_{\text{av}} \right\} \quad (3)$$

where P_{av} is the available active power that the generating units are able to supply.

This work was funded by the Research and Development project PD 2866-0468/2017, granted by the Agência Nacional de Energia Elétrica (ANEEL) and Companhia Paranaense de Energia (COPEL).

III. The Brazillian regulation on reactive power

In Brazil the absolute value of the power factor of an installation[1] should not be under 0.92 otherwise a penalty will be added to the energy bill [6].

The value to be paid in a given period M (usually one month), as specified in REN414/2010 [6] by ANEEL (*Agência Nacional de Energia Elétrica*) and considering only penalties due to the excessive consumption of reactive energy, is given by:

$$B_M = A_M + R_M, \tag{4}$$

where, B_M is the the total value of the energy bill, A_M is the portion due to the consumption of active energy and R_M are penalties due to the reactive excess.

The portion of the value due to the active power consumption is given by:

$$A_M = \sum_{H \in M} r_H E_H, \tag{5}$$

where r_H is the price of the energy during the period H (usually one hour), E_H is the active energy imported from grid during the same period.

The penalties due to low power factor are computed as:

$$R_M = \sum_{H \in F} r_H E_H \left(\frac{pf_{\text{ref}}}{pf_H} - 1 \right), \tag{6}$$

where $F \subseteq M$ is the set of intervals where the power factor was below the allowable value, pf_{ref} is the reference value for power factor, specified by ANEEL (at present time is 0.92) and pf_H is the mean power factor of the installation during the period H.

Using equations (5) and (6), the equation (4) can be redefined as

$$B_M = \sum_{H \in (M \setminus F)} r_H E_H + \sum_{H \in F} r_H E_H \left(\frac{pf_{\text{ref}}}{pf_H} \right). \tag{7}$$

IV. The proposed performance index

Based the equation (7), the instantaneous cost of the microgrid can be expressed as a function of the apparent power exchanged with the grid:

$$B(P_G, Q_G) = \begin{cases} r_H P_G, & \text{if } |pf(P_G, Q_G)| \geq pf_{\text{ref}} \\ r_H P_G \left(\dfrac{pf_{\text{ref}}}{pf(P_G, Q_G)} \right), & \text{otherwise} \end{cases}, \tag{8}$$

where P_G and Q_G are the active and reactive power imported from grid, respectively, and $pf(P_G, Q_G)$ is the instantaneous power factor, defined as:

$$pf(P_G, Q_G) = \frac{P_G}{\sqrt{P_G^2 + Q_G^2}} \tag{9}$$

[1]Only for installations fed with 2.3 kV or above.

However the equation (8) is a discontinuous function when exists a surplus of generation, i.e. $P_G < 0$, as shown by the limits:

$$\begin{aligned} B_{LHS} &= \lim_{pf(P_G,Q_G) \to -pf_{\text{ref}}^-} B(P_G, Q_G) = r_H P_G \\ B_{RHS} &= \lim_{pf(P_G,Q_G) \to -pf_{\text{ref}}^+} B(P_G, Q_G) = -r_H P_G \\ &\Downarrow \\ B_{LHS} &\neq B_{RHS} \end{aligned} \tag{10}$$

The value of B_{RHS} in (10) can be interpreted as an additional fee due the injection of active power into the grid, instead of a discount, showing a incoherent way to charge the energy.

To solve this inconsistency, and avoid the discontinuity that may cause a convergence problem for numerical methods, the function B has been redefined as:

$$B(P_G, Q_G) = \begin{cases} r_H P_G, & \text{if } |pf(P_G, Q_G)| \geq pf_{\text{ref}} \\ r_H P_G \left(1 + \dfrac{pf_{\text{ref}}}{pf(P_G, Q_G)} - \dfrac{P_G}{|P_G|} \right), & \text{otherwise} \end{cases}, \tag{11}$$

Removing the price r_H from expression (11), since it does not depend on the power consumption, and using (9), the performance index is defined as:

$$\mathcal{J}(P_G, Q_G) = \begin{cases} P_G, & \text{if } \alpha \\ pf_{\text{ref}} \sqrt{P_G^2 + Q_G^2}, & \text{if } \beta \\ pf_{\text{ref}} \sqrt{P_G^2 + Q_G^2} + 2P_G, & \text{otherwise} \end{cases} \tag{12}$$

where α and β are the conditions $|pf(P_G, Q_G)| \geq pf_{\text{ref}}$ and $|pf(P_G, Q_G)| < pf_{\text{ref}} \wedge P_G \geq 0$, respectively. This index can be interpreted as an equivalent value if all the consumption are only active power.

V. The analysis of the cost function

Substituting (1) in (12), it is possible to redefine the cost function J in terms of the power injected by the generating set and absorbed by the loads. Assuming that the power consumed by the loads can not be controlled, the cost function can be redefined as:

$$\mathcal{J}(P_D, Q_D) = \begin{cases} P_L - P_D, & \text{if } \alpha \\ P_R, & \text{if } \beta \\ P_R + 2(P_L - P_D), & \text{if } \gamma \end{cases} \tag{13}$$

where $P_R = pf_{\text{ref}} \sqrt{(P_L - P_D)^2 + (Q_L - Q_D)^2}$. α, β and γ are the the regions where $\{|pf(P_L - P_D, Q_L - Q_D)| \geq pf_{\text{ref}}\}$, $\{|pf(P_L - P_D, Q_L - Q_D)| < pf_{\text{ref}} \wedge P_L \geq P_D\}$ and $\{|pf(P_L - P_D, Q_L - Q_D)| < pf_{\text{ref}} \wedge P_L < P_D\}$, respectively. The Fig. 2 shows an example of contour lines for this cost function over the three interest regions α, β and γ. The Fig. 4a makes the division among this regions explicit.

The image of the cost function $\mathcal{J}$, considering its entire domain, does not have a stationary point, as shown by expression (14).

$$\forall (P_D, Q_D) \in \mathbb{R}^2 - \{(P_L, Q_L)\} : \nabla \mathcal{J} \neq \vec{0}. \tag{14}$$

The image of the cost function $\mathcal{J}$ is limited if its domain are constrained to the region $\mathcal{G} \cap \mathcal{T}$, this fact and the lack of

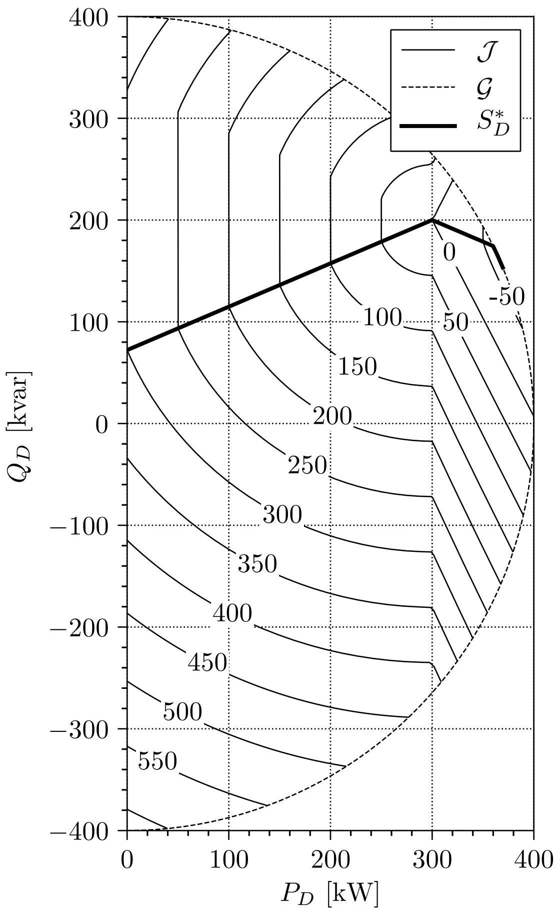

Fig. 2: Contour lines of the cost function $\mathcal{J}$ bounded by the constraint G and $\mathcal{T}$. Where $P_L = 300$ kW, $Q_L = 200$ kvar, $pf_{\text{ref}} = 0.92$ and $S_{\max} = 400$ kVA.

stationary points, implies that the pair $(P_D^*, Q_D^*) \to \min \mathcal{J}$ exists and are in set of limit points of the region $\mathcal{G} \cap \mathcal{T}$, according to the Weierstrass-Bolzano theorem.

VI. The Optimization Algorithm

The optimization process is divided into three stages. First, the optimization is performed only over the boundary region of $\mathcal{G}$, then it is evaluated if this solution satisfies the $\mathcal{T}$ constraint. If it is not satisfied, the optimization is performed over the superior limit of $\mathcal{T}$, and evaluated if this new solution satisfies $\mathcal{G}$. And if it is not satisfied, it is evaluated at the point of intersection between the boundary of $\mathcal{G}$ and the superior limit of $\mathcal{T}$. This process is shown in Fig. 3.

A. The algorithm to minimize $\mathcal{J}$ over $\mathcal{G}$

Since the minimum point of the cost function is on the border of operating region, this point can be obtained using the Lagrange multiplier method. This method assumes that, at a critical point of a function $f(x_1, ..., x_n)$ over given a equality condition $g(x_1, ..., x_n) = u$, the gradient vectors $\nabla f(x_1, ..., x_n)$ and $\nabla g(x_1, ..., x_n)$ are parallel:

$$\begin{cases} \nabla f(x_1, ..., x_n) = \lambda \nabla g(x_1, ..., x_n) \\ g(x_1, ..., x_n) = u \end{cases}, \tag{15}$$

where λ is a scalar. In this case, if $\lambda > 0$ the critical point is a maximum, and if $\lambda < 0$, this is a minimum point.

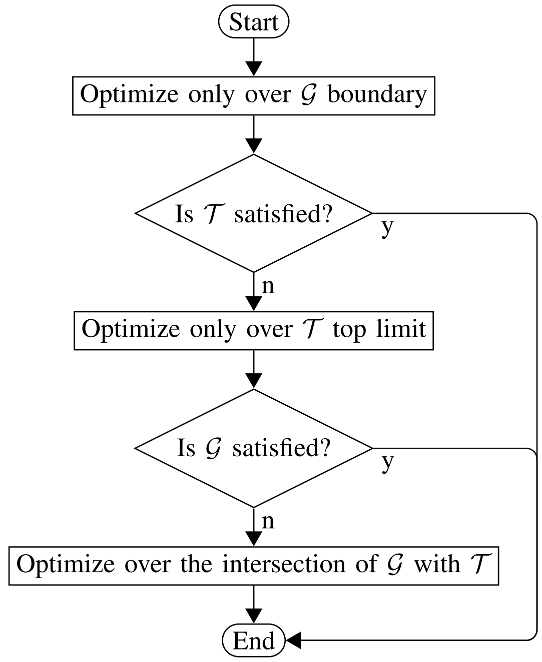

Fig. 3: General optimization algorithm.

As shown in (15), the optimization problem over the boundary of $\mathcal{G}$ is formulated as:

$$\begin{cases} \nabla \mathcal{J}(P_D, Q_D) = \lambda \nabla G(P_D, Q_D) \\ G(P_D, Q_D) = S_{\max} \end{cases}, \tag{16}$$

where $G(P_D, Q_D) = \sqrt{P_D^2 + Q_D^2}$.

The cost function, as described in (13), is piecewise-defined function characterized by three smooth functions $\mathcal{J}_\alpha$, $\mathcal{J}_\beta$ and $\mathcal{J}_\gamma$, whose domain are limited to the regions α, β and γ, respectively. The Figs. 4b, 4c and 4d show these functions separately, but constrained only by $\mathcal{G}$.

The first step in this algorithm is to find the pairs $S_{D\alpha}^*$,$S_{D\beta}^*$ and $S_{D\gamma}^*$ that minimize functions $\mathcal{J}_\alpha$, $\mathcal{J}_\beta$ and $\mathcal{J}_\gamma$, respectively, over the entire $\mathcal{G}$ region. This points are obtained the Lagrange multiplier method, as described in (16), and can defined as:

$$S_{D\alpha}^* = (S_{\max}, 0); \tag{17}$$

$$S_{D\beta}^* = \left(\frac{S_{\max}}{|S_L|} P_L, \frac{S_{\max}}{|S_L|} Q_L \right); \tag{18}$$

$$S_{D\gamma}^* = \text{Solved using Newton-Raphson.} \tag{19}$$

If $S_{D\alpha}^*$ is in α, then it is returned as the global minimum point of $\mathcal{J}$ over $\mathcal{G}$, and the algorithm ends.

If $S_{D\beta}^*$ is in β and P_L is greater than $S_{\max}$, it implies that the γ region is an empty set, then $S_{D\beta}^*$ is returned as the minimum point and the algorithm ends.

If $S_{D\gamma}^*$ is in γ and $S_{D\beta}^*$ is not in β region, then $S_{D\gamma}^*$ is the only valid critical point, it is returned and the algorithm ends.

If $S_{D\gamma}^*$ is in γ and $S_{D\beta}^*$ is in β region, then both $S_{D\beta}^*$ and $S_{D\gamma}^*$ are valid critical points. The algorithm returns the one that minimizes the value of $\mathcal{J}$ and the algorithm ends.

If $S_{D\beta}^*$ is in α and $S_{D\alpha}^*$ is in β, it implies that neither $S_{D\alpha}^*$ nor $S_{D\beta}^*$ are valid critical points. In this case the minimal

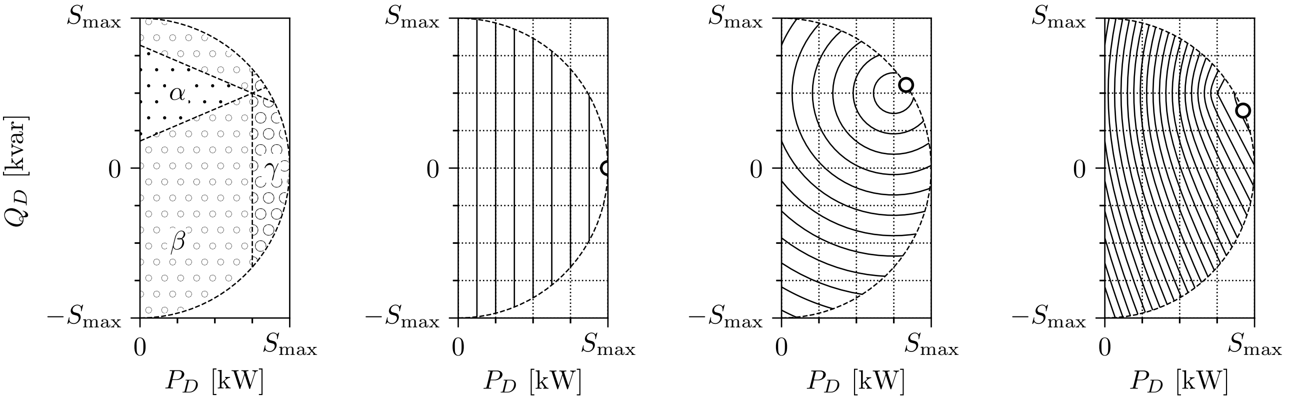

(a) (b) $\mathcal{J}_\alpha$ (c) $\mathcal{J}_\beta$ (d) $\mathcal{J}_\gamma$

Fig. 4: Characteristics of cost function $\mathcal{J}$. (a) The division of $\mathcal{G}$ into regions α, β and γ. (b) $\mathcal{J}_\alpha$. (c) $\mathcal{J}_\beta$. (d) $\mathcal{J}_\gamma$. Where $P_L = 300$ kW, $Q_L = 200$ kvar, $pf_{\text{ref}} = 0.92$ and $S_{\max} = 400$ kVA. All values of the contour lines correspond to the values of the contour shown in Fig. 2, according to their respective regions.

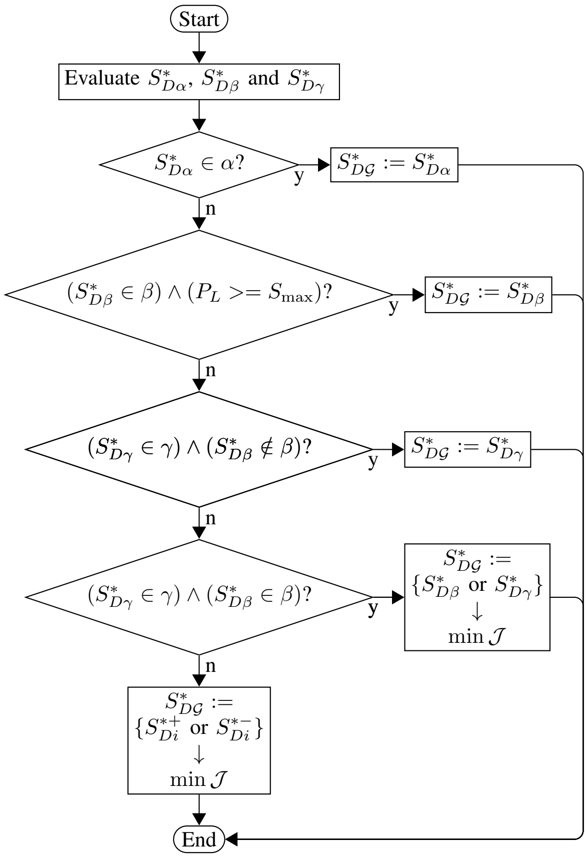

Fig. 5: Optimization algorithm over $\mathcal{G}$.

point are at the border of $\mathcal{G}$ in the frontier between α and β regions. The same applies if $S^*_{D\gamma}$ is in α and $S^*_{D\alpha}$ is in γ. This S^*_{Di} intersection point is defined as:

$$\begin{cases} S^*_{Di} = (P^*_{Di}, Q^*_{Di}) \\ P^*_{Di} = \frac{k(kP_L \pm Q_L) + \sqrt{(1+k^2)S^2_{\max} - (kP_L \pm Q_L)^2}}{(1+k^2)} \\ Q^*_{Di} = Q_L \pm k(P_L - P^*_{Di}) \\ k = \dfrac{\sqrt{1 - pf^2_{\text{ref}}}}{pf_{\text{ref}}} \end{cases}, \tag{20}$$

where the operator $\pm$ must be replaced by $+$ or $-$ over the entire system of equations. It will result in only two points: S^{*+}_{Di}, if all $\pm$ are replaced by $+$; and S^{*-}_{Di}, if all $\pm$ are replaced by $-$. In this definition, one of those two points may not exist if the conditions lead to a negative value inside the square root, in the P^*_{Di} definition.

If both S^{*+}_{Di} and S^{*-}_{Di} exist, is chosen the one that minimizes $\mathcal{J}$ otherwise, the only existing point are returned and algorithm ends.

The entire algorithm is illustrated in Fig. 5.

B. The algorithm to minimize $\mathcal{J}$ over $\mathcal{T}$

The minimum value of $\mathcal{J}$ along the line $P_D = P_{\text{av}}$ occurs over the region of intersection between the line $P_D = P_{av}$ and α. This results in an set of possible minimum points. To select only one point $S^*_{D\mathcal{T}}$ in this set, a minimum effort strategy is used. This strategy aims at the conservation of the equipment, setting the active power at the maximum available and selecting the absolute minimum value for the reactive power that allows the operation on the alpha region. This minimum point is defined by:

$$S^*_{D\mathcal{T}} = \begin{cases} (P_{\text{av}}, 0) & \text{if } (P_{\text{av}}, 0) \in \alpha \\ (P_{\text{av}}, Q_L - k(P_L - P_{\text{av}})) & \text{if } (P_{\text{av}}, 0) \notin \alpha \wedge \\ & (Q_L >= 0 \wedge P_L >= P_{\text{av}} \vee \\ & Q_L < 0 \wedge P_L < P_{\text{av}}) \\ (P_{\text{av}}, Q_L + k(P_L - P_{\text{av}})) & \text{if } (P_{\text{av}}, 0) \notin \alpha \wedge \\ & (Q_L >= 0 \wedge P_L < P_{\text{av}} \vee \\ & Q_L < 0 \wedge P_L >= P_{\text{av}}) \end{cases} \tag{21}$$

where k is as defined in (20).

C. The algorithm to minimize $\mathcal{J}$ over the intersection of the boundary of $\mathcal{G}$ and $\mathcal{T}$

This algorithm find the intersection between the line $P_D = P_{\text{av}}$ and the circle G, as described in (16) and selects the point that minimizes $\mathcal{J}$. The minimal point is defined as:

$$S^*_{D\mathcal{G}\mathcal{T}} = \begin{cases} (P_{\text{av}}, \sqrt{S^2_{\max} - P^2_{\text{av}}}) & \text{if } Q_L > 0 \\ (P_{\text{av}}, -\sqrt{S^2_{\max} - P^2_{\text{av}}}) & \text{if } Q_L < 0 \end{cases}. \tag{22}$$

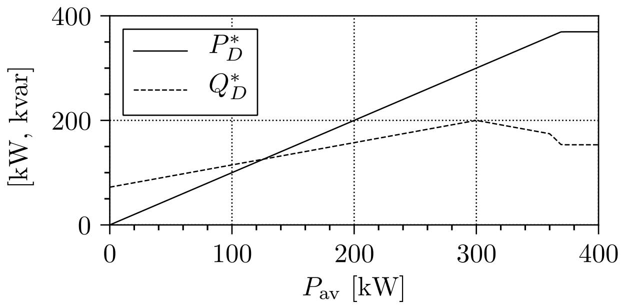

Fig. 6: Evolution of the optimal active P_D^* and reactive Q_D^* power as the available active power P_{av} increases. Where $P_L = 300$ kW, $Q_L = 200$ kvar, $pf_{\mathrm{ref}} = 0.92$ and $S_{\max} = 400$ kVA.

VII. Results

The Fig. 6 shows an example of how the optimal point evolves as more active power are available at the primary source. In this figure, the active power supplied by the generation group are limited, even though more power is available at the primary source. It occurs in way to prevent a degradation of the power factor due to a small value of active power P_G exchanged between the microgrid and the public grid. The optimal path of S_D^* are shown in Fig. 2.

To test the performance of the proposed method, a simulation was made using the data shown in Fig. 7.

The Fig. 9 shows the power factor without any generation, with generation but without any reactive compensation, and with generation using the proposed method to control the reactive and active power dispatch. In this figure, are clear the degradation of the power factor (even when the loads do not have power factor problems) due to low active power flowing to/from the main grid when the generation is close to equilibrium with the active power consumed. This figure also shows how the proposed method helps to maintain the power quality of the microgrid.

In Fig. 8 are shown the difference between the maximum active power strategy and the proposed method. It confirms that the proposed method will lead to a cost equal or lower than the maximum active power strategy. The cumulative value shows the total economy (in equivalent real energy) provided by the proposed method.

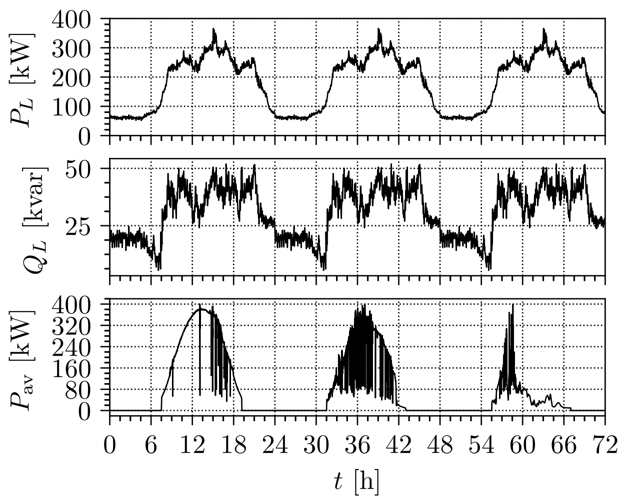

Fig. 7: Consumption and generation data used in simulation.

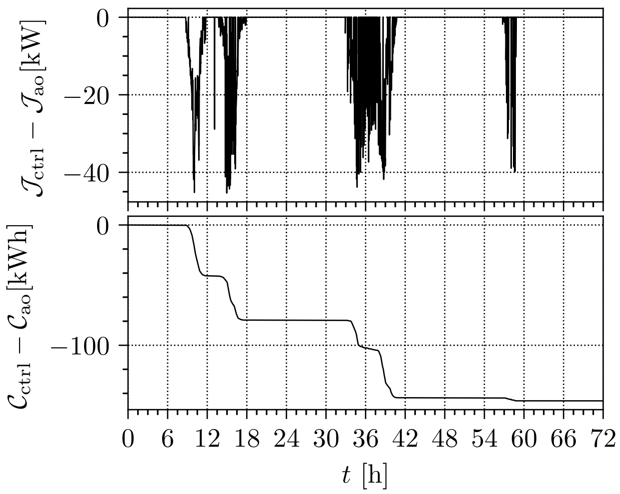

Fig. 8: The instantaneous value of the cost function $\mathcal{J}_{\mathrm{ctrl}}$, and the cumulative value C_{ctrl} and, for comparison, the values using the maximum active power export strategy, $\mathcal{J}_{\mathrm{ao}}$ and C_{ao}.

TABLE I: Duration of some events over the entire simulation.

	Active Power Only	**Proposed Method**
Power factor degraded	15.30%	4.08%
Power factor critically degraded (under 99.9% of pf_{ref})	15.18%	0.00%
Active power below max	0.00%	0.00%
Non-zero reactive power	0.00%	15.30%

VIII. Conclusion

The proposed method performed a sensible minimization of the instantaneous cost, and this minimization becomes more apparent as the natural power factor of the installation (without distributed generation) becomes more degraded.

The results showed an improvement in the power factor, when the generation exceeds the active power consumption, without exclusively compensating the reactive power. The result also shows that the algorithm do not aim a unitary power factor, it only tends to stabilize close to the limit between the normal and degraded power factor regions.

The separation of the cost function into multiple smooth functions allowed a stable and fast numerical convergence, and setting a constant iteration number for the Newton-Raphson method, the algorithm has a time complexity $O(1)$. This fact allows the algorithm to be implemented in a real-time solution.

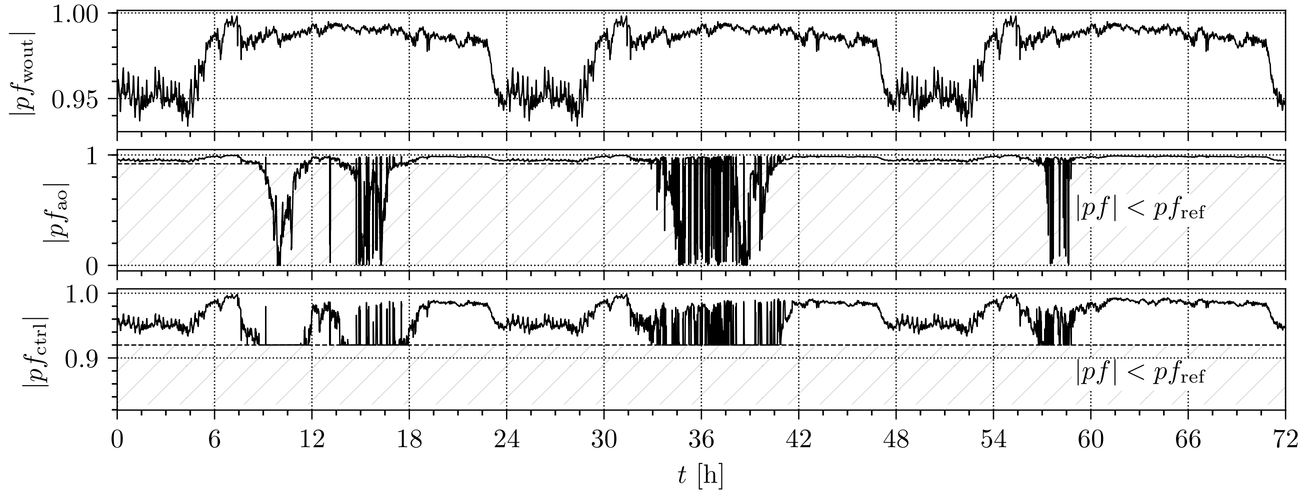

Fig. 9: Absolute value of power factor of the microgrid; without distributed generation $|pf_{\mathrm{wout}}|$; with distributed generation, but only injection the maximum active power available and no reactive $|pf_{\mathrm{wout}}|$; and using the proposed method $|pf_{\mathrm{ctrl}}|$. Where $pf_{\mathrm{ref}} = 0.92$ and $Smax = 450$ kVA.

ACKNOWLEDGMENT

This work was partially funded by the Research and Development project PD 2866-0468/2017, granted by the Brazilian Electricity Regulatory Agency (ANEEL) and Companhia Paranaense de Energia (COPEL). The authors also thank to FINEP, CAPES, SETI, CNPq, Fundação Araucária and UTFPR for scholarships and additional funding

REFERENCES

[1] R. Lasseter, "MicroGrids," in *2002 IEEE Power Engineering Society Winter Meeting. Conference Proceedings (Cat. No.02CH37309)*, vol. 1. IEEE, 2002, pp. 305–308.

[2] F. Katiraei and M. R. Iravani, "Power Management Strategies for a Microgrid With Multiple Distributed Generation Units," *IEEE Transactions on Power Systems*, vol. 21, no. 4, pp. 1821–1831, nov 2006.

[3] H. Bevrani, B. Francois, and T. Ise, *Microgrid dynamics and control*. Hoboken: John Wiley and Sons Ltd, 2017.

[4] P. P. Vergara, H. R. Shaker, B. Norregaard, and L. C. P. da Silva, "Distributed consensus-based economic dispatch considering grid operation," in *2017 IEEE Power Energy Society General Meeting*, July 2017, pp. 1–5.

[5] M. P. Contzen and J. Raisch, "Reactive power consensus in microgrids," in *2016 European Control Conference (ECC)*, June 2016, pp. 334–339.

[6] ANEEL, "Resolução Normativa Nº 414 de 9 setembro de 2010. Estabelece as Condições Gerais de Fornecimento de Energia Elétrica de forma atualizada e consolidada," *Diário Oficial da União*, 15 set. 2010. [Online]. Available: http://www2.aneel.gov.br/cedoc/ren2010414.pdf